ZnO Transparent conductive oxide for thin film silicon solar cells

T. Söderström, D. Dominé, A. Feltrin, M. Despeisse, F. Meillaud, G. Bugnon, M. Boccard, P. Cuony, F.-J. Haug, S. Faÿ, S. Nicolay and C. Ballif
École Polytechnique Fédérale de Lausanne (EPFL), Institute of Microengineering (IMT), Thin Film Electronics Laboratory, Rue A.-L. Breguet 2, CH-2000 Neuchâtel, Switzerland

ABSTRACT

There is general agreement that the future production of electric energy has to be renewable and sustainable in the long term. Photovoltaic (PV) is booming with more than 7GW produced in 2008 and will therefore play an important role in the future electricity supply mix. Currently, crystalline silicon (c-Si) dominates the market with a share of about 90%. Reducing the cost per watt peak and energy pay back time of PV was the major concern of the last decade and remains the main challenge today. For that, thin film silicon solar cells has a strong potential because it allies the strength of c-Si (i.e. durability, abundancy, non toxicity) together with reduced material usage, lower temperature processes and monolithic interconnection. One of the technological key points is the transparent conductive oxide (TCO) used for front contact, barrier layer or intermediate reflector. In this paper, we report on the versatility of ZnO grown by low pressure chemical vapor deposition (ZnO LP-CVD) and its application in thin film silicon solar cells. In particular, we focus on the transparency, the morphology of the textured surface and its effects on the light in-coupling for micromorph tandem cells in both the substrate (n-i-p) and superstrate (p-i-n) configurations. The stabilized efficiencies achieved in Neuchâtel are 11.2% and 9.8% for p-i-n (without ARC) and n-i-p (plastic substrate), respectively.

Keywords: Transparent conductive oxide, ZnO, light trapping, thin film silicon solar cells

1. INTRODUCTION

Solar energy conversion has the potential to satisfy the electricity and even the total energy consumption of the world. Indeed, one hour of solar irradiation on earth is equivalent to the total world energy consumption in one year (about 130 PWh). Photovoltaic (PV) or the direct conversion of sunlight into electricity is a promising technology which can be easily installed without affecting neither the landscape nor the natural environment if directly integrated into building (BIPV). Strong effort has been made in the past decade to decrease the cost per Watt peak of PV. Indeed, the standard crystalline silicon technology, which had a 90 % market share in year 2008, saw a decrease in production cost by a factor of 20 in 30 years. Further cost reduction can be made by using thinner films which use less material and large area monolithic integration while keeping the advantages of silicon, i.e. durability, abundancy, non toxicity [1]. These thin Si films can be grown by plasma enhanced chemical vapor deposition (PECVD) on rough conductive substrates[2]. The roughness is necessary to scatter the light and enhance the light in-coupling in the thin solar cells (0.1-10 μm). In this paper, we report on the versatility of ZnO deposited by low pressure chemical vapor deposition (LP-CVD). The LP-CVD process can produce transparent, textured, highly conductive films or flat non conductive films depending on the growth temperature. Furthermore, we implement these films as transparent conductive oxide for front contact and intermediate reflector for both substrate (n-i-p) and superstrate (p-i-n) configuration thin film silicon solar cells.

The micromorph tandem solar cell, composed of an amorphous silicon (a-Si:H) top cell and a microcrystalline silicon (μc-Si:H) bottom cell [3], is one of the most promising multi-junction candidates for thin film silicon solar cells with high stabilized efficiency. Indeed, the combination of a high a-Si:H band gap (1.7 eV) and a low μc-Si:H band gap (1.1 eV) creates an almost ideal tandem device[4]. The challenge of this device is to achieve ideal short circuit current density (Jsc) matching between the two sub cells because in multi-junction solar cells, the Jsc is limited by the lowest Jsc of the sub cells. In micromorph tandem cells where an amorphous cell is stacked on top of a microcrystalline cell, the light passes through the top cell only once; the weakly absorbed light will pass into the bottom cell and is eventually absorbed there as shown in Figure 1 (B). The light induced degradation[5] forbids the use of thick a-Si:H solar cells [6,7]. Therefore, in tandem micromorph cells, the limitation in Jsc comes usually from the top cell. One widely used solution in the superstrate configuration (p-i-n) is to introduce a thin intermediate reflector (IR)[8] which enhances the Jsc of the top cell

Oxide-based Materials and Devices, edited by Ferechteh Hosseini Teherani, David C. Look, Cole W. Litton, David J. Rogers, Proc. of SPIE Vol. 7603, 76030B

without the need of increasing its absorber layer thickness. The IR is usually a material with a refractive index lower than silicon (typically, at a wavelength of 600 nm: $1.5 < n_{IR} < 3$ compared to $n_{Si} \sim 4$) in order to have an index contrast that increases the reflection of the light at the Si/IR interface as presented. Therefore, it enhances the Jsc of the top cell without increasing its thickness. The IR is usually a thin layer, between 50 and 150 nm, deposited in-situ or ex situ. In situ Silicon Oxide Intermediate Reflector (SOIR), Silicon Nitride or ex situ Zinc Oxide Intermediate Reflector (ZIR) have been reported to be very effective and are already implemented in complete products[9]. In the superstrate configuration, the light incoupling is driven by the texture of the front contact. Here, we present two type of front contact, type A and B with small and large feature size, respectively. In addition, we also present the effect of the resistivity of the IR on the solar cell electrical performances (V_{oc} and FF). In the substrate configuration (n-i-p), the efficiency limitation comes also from the top cell current density and therefore we compare conformal and asymmetric reflector in the solar cells.

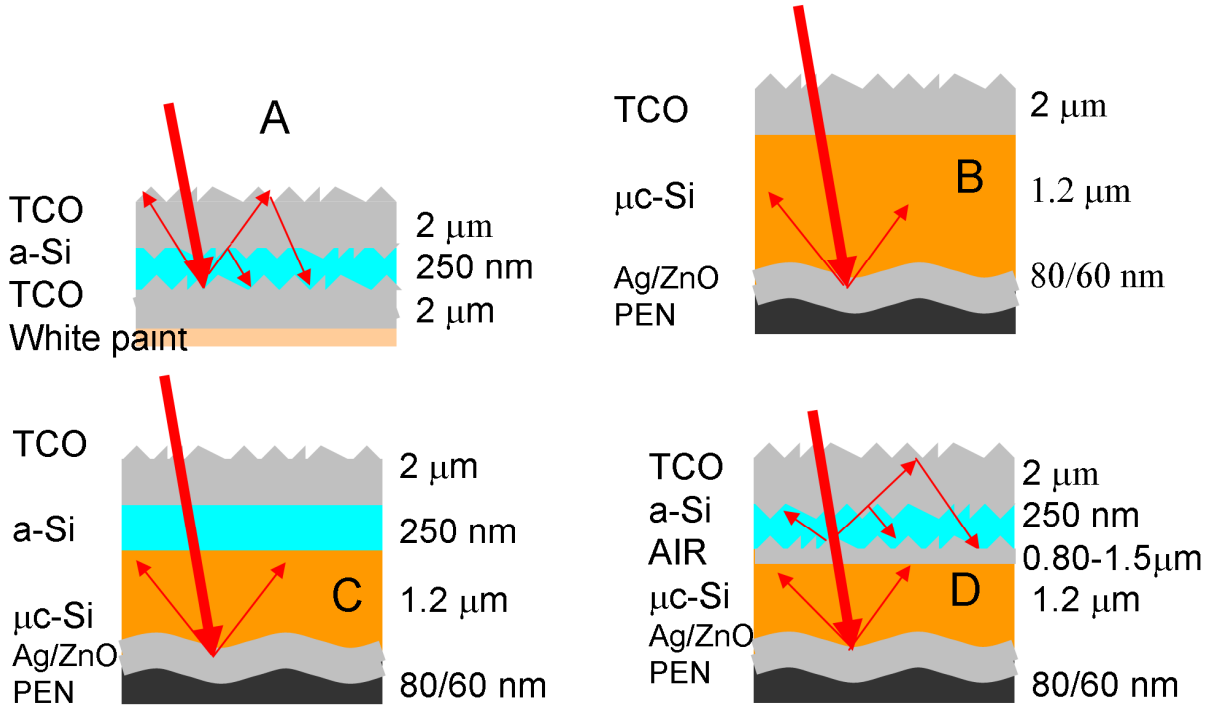

Figure 1: Schema of single junction a-Si:H (A), single junction µc-Si:H (B), tandem micromorph a-Si:H/µc-Si:H (C) and tandem micromorph with asymmetric intermediate reflector (D) deposited on textured substrates covered with thin Ag/ZnO.

2. EXPERIMENTAL

2.1 ZnO LP-CVD

ZnO films were deposited by LPCVD process on 4 by 4 cm^2, 0.5mm thick AF45 Schott glass substrates. Before deposition, the substrates were chemically cleaned with acid and base in ultrasonic baths. Diethylzinc (DEZ) and water (H_2O) vapors were used as precursors. Diborane (B_2H_6) was used as doping gas, diluted at 1% in argon. The total pressure was kept at 0.3 mbar inside the reactor and the growth temperature was varied from 110 to 200 °C. The different samples were characterized with transmission electron microscopy and scanning electron microscopy to study, respectively, the film crossection and the surface morphology.

2.2 Thin film solar cells

The design of thin film silicon solar cells is determined by the electronic properties of the amorphous and microcrystalline layers. Since doping drastically reduces diffusion length, doped layers are not photoactive. Therefore their role is to create an electric field in the photoactive intrinsic layer sandwiched between the two doped layers. Depending whether the substrate being used for silicon deposition is transparent or not, two different sequences of layer stacking are used in thin film silicon technology.
Figure **2** shows the two possible configurations. In the first one, called superstrate (p-i-n) configuration, the substrate is glass. In the second one, called substrate (n-i-p) configuration, the substrate is opaque like a plastic or metal and if the sheet is thin enough, flexible solar cells can be obtained.

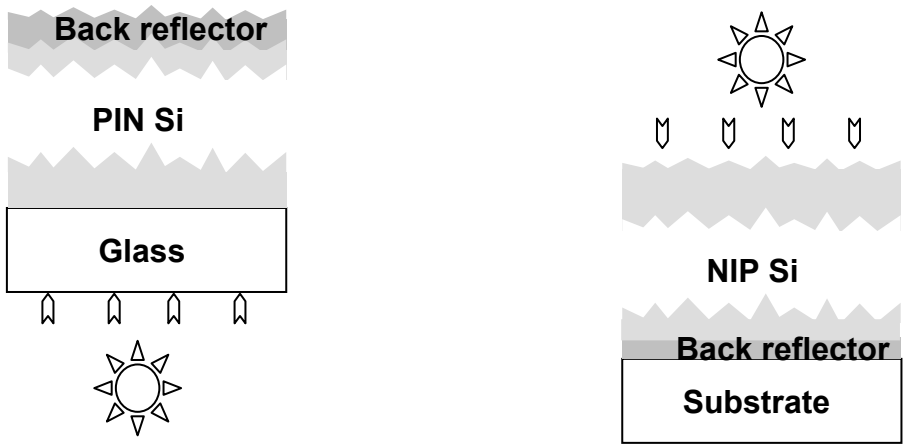

Figure 2: Sketches of thin film silicon cells in superstrate (left) and substrate (right) configurations.

The superstrate (p-i-n) cells are grown on AF45 borosilicate glass substrates from Schott. First, the substrates are covered with a transparent front contact of LPCVD-ZnO; two different conditions are used, strongly doped films with a thickness of 1.9 μm (type A), and lightly doped films with a thickness of 4.8 μm (type B)[10]. The sheet resistance of both substrates is 10 Ω/sq, their surface roughnesses are 66 and 180 nm RMS (root mean square roughnesss), respectively. The thicker ZnO layer is subjected to a plasma treatment which changes the initial V-shaped morphology to U-shaped morphology which is better suited for the growth of microcrystalline silicon (type C) [11]. Depending on the duration of the treatment, the roughness can be reduced as much as down to 120 nm rms [12]. The amorphous and microcrystalline layers are deposited by very high frequency plasma enhanced chemical vapor deposition (VHF-PECVD) under similar conditions to those of the previous section. The intermediate reflector in the presented p-i-n cells is made from n-doped SiOx (SOIR) by in-situ processing [13] or excitu by a low conductivity ZnO LP-CVD process [8]. The back contact of the p-i-n cells consists again of LPCVD-ZnO covered with a white reflector.

The substrate (n-i-p) cells presented here have been grown on a flexible polyethylene (PEN) substrate. The surface of the substrate is textured with a periodic sinusoidal structure which is embossed into the surface by a roll-to-roll process [14]. The substrate is covered conformally by sputtering of a bilayer of silver and zinc oxide with thicknesses of 80 and 60 nm, respectively. The silicon layers are deposited by VHF-PECVD from a mixture of silane (SiH_4) and hydrogen (H_2). Phosphine (PH_3) and tri-methyl-boron ($B(CH_3)_3$) are used as doping gases. The front contact consists of a 3.8 μm thick ZnO layer deposited by low pressure CVD (LP-CVD) which results in naturally textured growth [15]. The layer is lightly boron doped in order to suppress free carrier absorption [11]. In the n-i-p tandem cells shown here we use the same LP-CVD process but without any intentional doping for the deposition of the intermediate ZnO reflector with a thickness of 1-2 μm [16].

The current voltage characteristics of all cells are measured under illumination with a dual source sun simulator (Wacom, Class A) in standard test conditions (25°C, AM1.5g spectrum, 100 mW/cm2). The current is determined independently by a measurement of the external quantum efficiency (EQE). Red and blue light bias are applied for

measuring top- and bottom cells, respectively, and the photocurrent is determined by integration of the EQE weighted by the spectral photon density of the AM1.5g spectrum.

3. RESULTS

3.1 ZnO LP-CVD

The transparent conductive oxide used in thin film solar cells need to be transparent and textured to ensure maximum transmitted and scattered light in the photovoltaic device. However, the growth of the ZnO LP-CVD depends strongly on the process temperature. In fact, the temperature changes the growth mechanism as presented by S. Nicolay in ref[17]. In Figure 3, the layer deposited at 110°C has only small grains. This is typical of polycrystalline film deposited under condition of low adatom surface diffusion[17]. These films have a poor lateral conductivity and no textured interface. Therefore, they are poor candidate as front TCO in the solar cells but they are of high interest as intermediate reflector where a low in plane conductivity reduces the undesired current drains in the cells. The layer deposited at 150°C, Figure 3 (right) has completely different grain structure with an incubation layer composed of small grains and the development of large columnar grains thanks to the higher diffusion of the adatoms at the surface of the films. The roughness achieved with these films is related with the thickness of the films and with the scattering power of the films as shown by J. Steinhauser in [18].

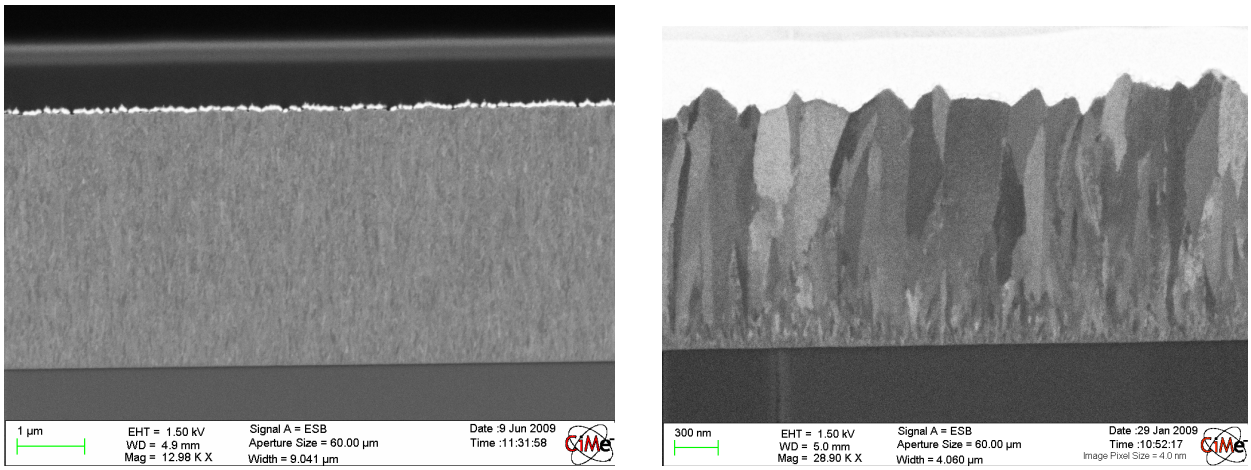

Figure 3: Two temperature deposition of ZnO LP-CVD layer. The layer on the left is deposited at 110°C and has small grains whereas the layer on the right is deposited at 150°C and has large grains.

Figure 4 shows the transmission (T), reflection (R) and absorption (A) curves of ZnO LP-CVD and ZnO LP-CVD covered with an index matching liquid CH_2I_2[19]. The ZnO is deposited on glass at 180 °C. This provides a natural texture close to the one shown on the right of Figure 3. When no matching liquid and cover glass is used, the textured ZnO provides diffuse transmittance, which is negligible in the case of ZnO measured with CH_2I_2. The rough interface of the ZnO leads to an increase of the absorbance between 400 to 600 nm and reflection between 500 to 1000 nm. Enhanced absorption is attributed to light trapping in the 2 µm thick ZnO due to scattering of the light at the air/ZnO interface and internal reflection between the glass/air and the ZnO/air interface. It enhances the path of the light in the ZnO and increases absorption due to residual optical defects and free carrier absorption, whereas the reflectance is increased because incident angle of the light on the flat ZnO/glass interface is increased. This TCO/glass structure does not give direct information on the optical behavior in the solar cell (TCO/Si) because light trapping due to total internal reflection will not take place for the TCO/Si interface ($n_{Si} > n_{TCO}$, which is different from $n_{TCO} > n_{glass}$ at the TCO/glass interface) and, therefore, complete solar cell has to be made to evaluate the effect of the texture as shown in the next sections. Note, that the Haze (defined as ration between diffuse and total transmission DT/T) of the textured ZnO is 85% at 400 nm and only 12% at 800 nm. Hence, in air the scattering power of our textured ZnO is limited for the infra-red (IR) part of the spectrum whereas in the device it has a high scattering power due to the stronger index contrast between silicon (n=4) and ZnO (n=1)[10].

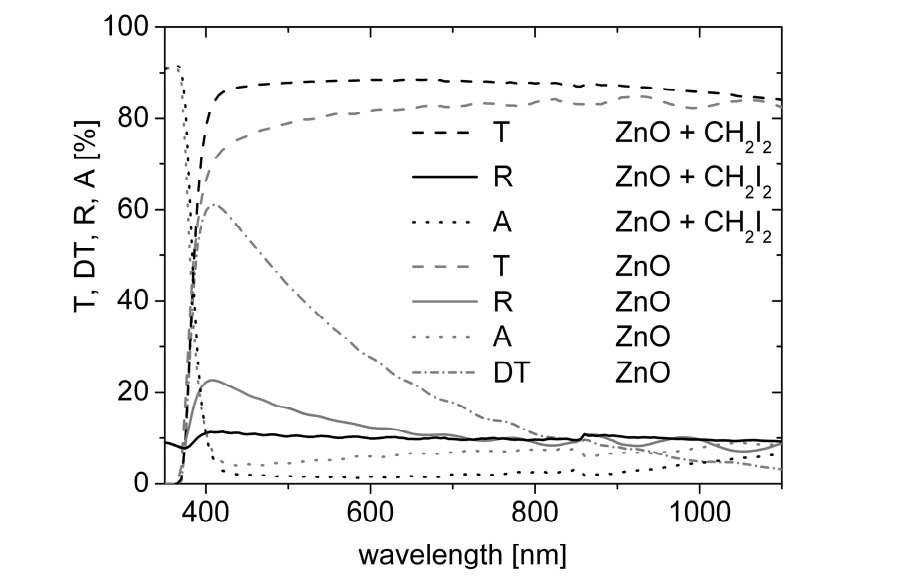

Figure 4: The reflection (R), transmission (T), diffuse transmission (DT) and absorption spectra of standard LP-CVD deposited at 180°C are presented. The solid line are the spectra for a film covered a index matching layer (CH2I2) which removes the effect of the texture.

3.2 Thin film silicon solar cells on glass

The p-i-n cell development is carried out on glass substrates covered with an LPCVD-ZnO front contact. Figure 5 shows typical surface morphologies for type A and type C substrates. Type A substrates consist of randomly distributed pyramids with a typical lateral feature size of 300 nm and clearly defined facets, whereas the surface treated type C substrates consist of large features (about 800 to 100 nm) with rounded out bottoms of U-shape.

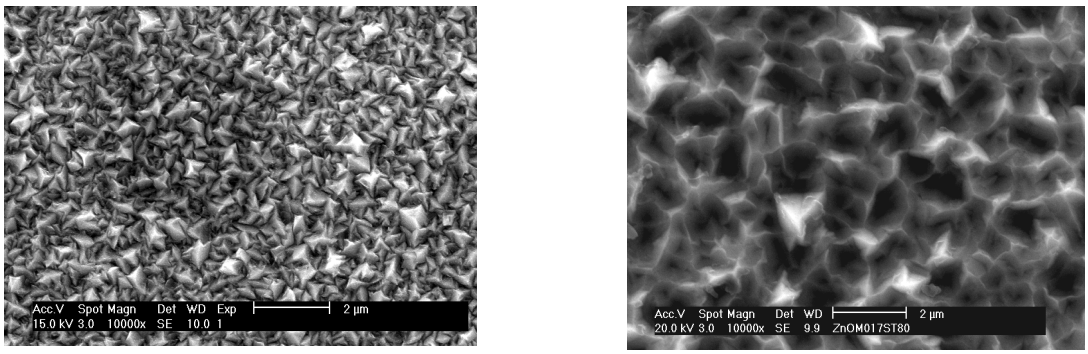

Figure 5: Surface morphology of type A (left) and type C (right) LPCVD-ZnO substrates.

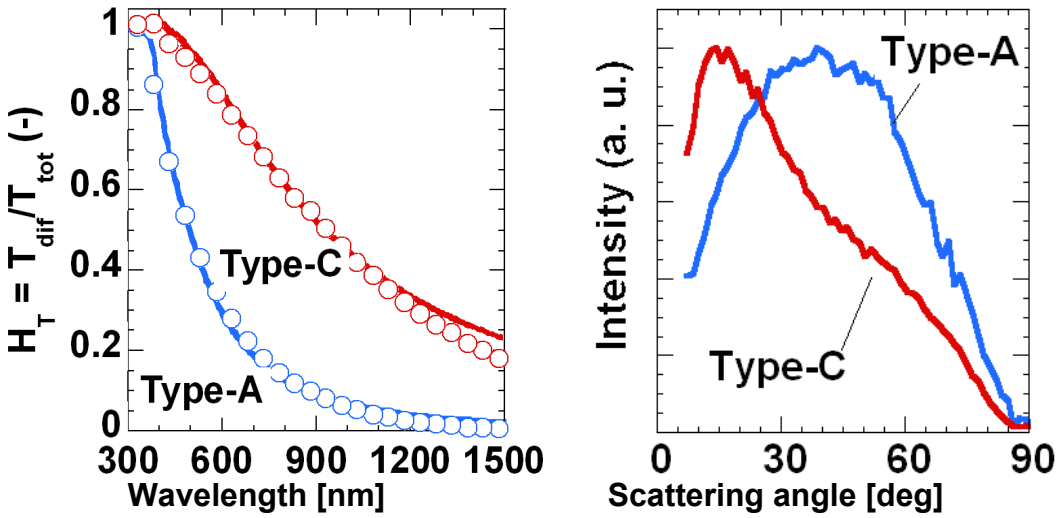

Figure 6: Spectral haze in transmission $H=R_{diff}/R_{tot}$ (left) and sin-weighted angular resolved scattering (ARS) characteristics of the type A and type C substrates (measured with transmission into air)

Figure 6 compares optical characteristics of the two layers; type A substrates show a haze function which decreases rapidly between 400 and 600 nm whereas on type C substrates the diffusion extends well into the IR range. However, the sin-weighted angular resolved scattering data in the right panel of Figure 6 shows that the type A substrate shows a maximum at 40° which is very close to the behavior of an ideal Lambertian diffuser (maximum at 45°), whereas the type C substrate scatters into a narrow angular distribution, the most probable scattering being only 15°.

Figure 7 compares EQEs of tandem cells on the two different types of LPCVD ZnO front contacts; the top and bottom cell thicknesses are 290 nm and 3.0 µm, respectively. The cells without intermediate reflector in the left panel show identical top cell currents of 10.9 mA/cm2, but the moderately doped type C substrate yields better bottom currents because of lower free carrier absorption in the TCO. We conclude that we have little light scattering at the TCO/Si interface, and the top current is essentially produced in one single pass through the amorphous absorber. The right panel compares the situation after the introduction of a SOIR with 150 nm thickness. Both top cells gain in current because of reflection at the SOIR, but we observe a larger gain in the device with the type A front contact (2.6 mA/cm2 compared to 2.1 mA/cm2 on the type C substrate). We can understand the observations in terms of the optical measurements shown in Figure 6 when we assume that the broad ARS of the type A substrate can offset its lower haze values. We have to keep in mind though, that the optical measurements in air are different from the situation in the cell where the actual scattering interface is between ZnO and silicon, not between ZnO and air. The best electric performance of a tandem cell deposited on glass without antireflection coating (ARC) with SOIR on the type C substrate has an initial efficiency of 12.6% which stabilizes at 11.2% after 1000 h of light soaking.

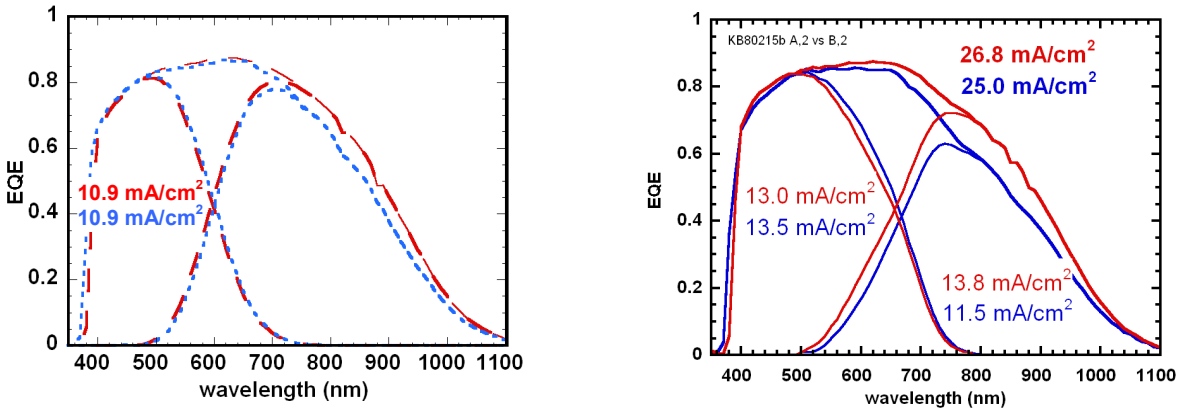

Figure 7: External quantum efficiencies of tandem solar cells on type A and type C substrates; left: no SOIR, right: with 150 nm thick SOIR.

So far the ZnO LP-CVD has been used as front contact and the SOIR was used as IR. The ZnO LP-CVD can also be used as IR (ZIR) as shown in Figure 8. Indeed, it was shown by D. Dominé that ZIR has similar optical properties that the SOIR [20]. However by implementing the same high conductive ZnO used for front contact as IR, we observe usually a reduction of V_{oc} and FF as shown in Figure 9. For IR, the resistive ZnO deposited at lower temperature is much more adapted because it avoids connecting the shunts of our device as demonstrated by D. Dominé in ref. [20].

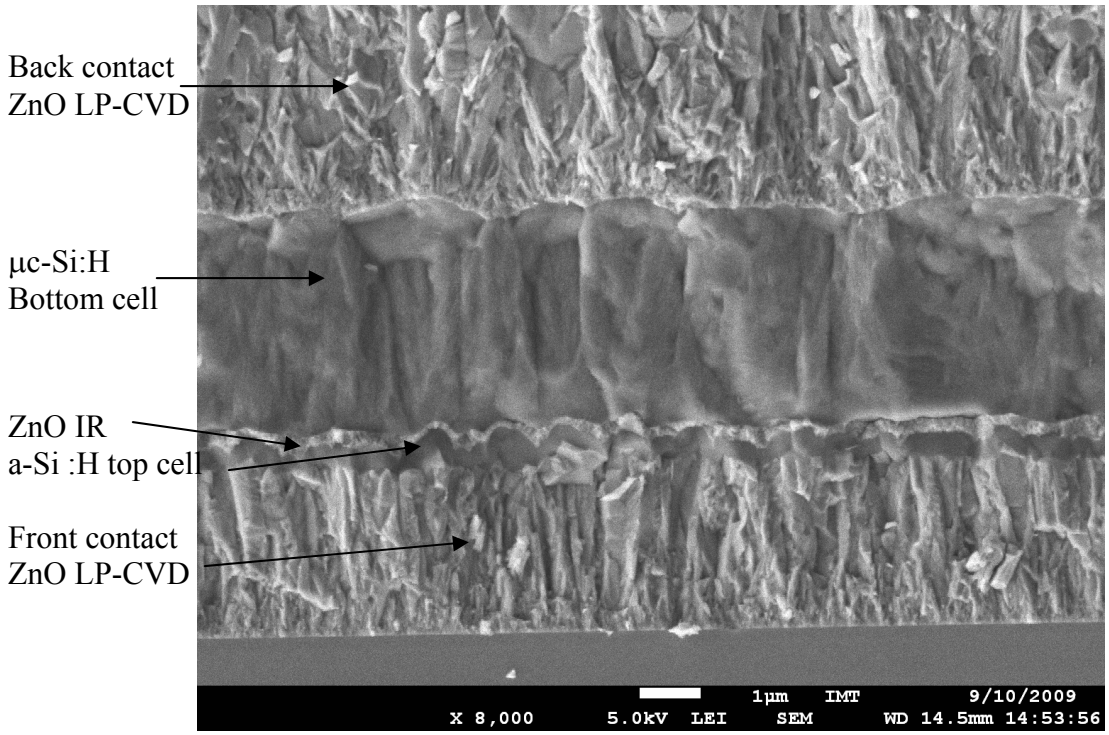

Figure 8: SEM cross section of micromorph tandem cell with ZnO intermediate reflector.

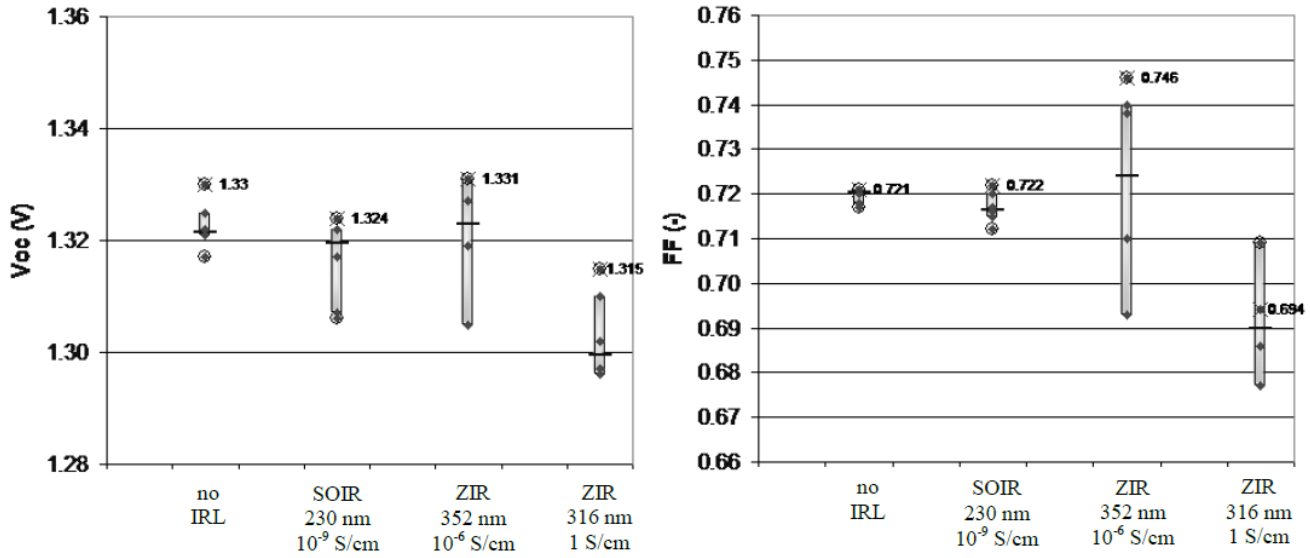

Figure 9: Result of the co-deposition run, for comparison of SOIR versus ZIR: comparison of (a) Voc and (b) FF of the co-deposited micromorph cells, without, and with, the insertion of an IRL (SOIR or ZIR with in-plane conductivity of 10-6 or 1 S/cm). For each of the 4 configurations, there is one substrate with 6 cells of 1.2 cm2 surface area. The graphs display the results of the measurements in the form of box-plots. For each set of 6 cells, the horizontal line is the median and the ends of the box are the first and third quartile of the set of data. For the cell with the best Voc on each substrate, the numerical values of Voc and FF are indicated.

3.3 Thin film silicon solar cells on plastic substrates (n-i-p)

Here, we present the results of n-i-p micromoph tandem cells without an intermediate reflector between the top and bottom cells. It was previously shown [21] that the growth of the μc-Si:H absorber reduces the texture of the substrate which consequently reduces the possibility of light scattering in the top cell. The light induced degradation of a micromorph tandem is mainly driven by the increase in defect density in the a-Si:H material. Indeed, there is an optimum between the reduction of the top cell thickness and the light-induced degradation of the tandem, which partly is driven by the decrease of J_{sc} of the a-Si:H cell as shown in Table 1. It shows, as expected, that the thicker the a-Si:H absorber, the higher the degradation of the micromorph cells; it is almost 20% cell with thick (300nm-600 nm) a-Si:H absorber and only 13% for 160 nm.

Table 1 : Initial and stable (in parentheses) parameters of the n-i-p micromorph tandem solar cells with various thicknesses of the a-Si:H top cell. The substrates for these micromorph cells are hot silver.

a-Si :H [nm]	V_{oc} [V]	FF [FF]	J_{top} [mA/cm^2]	J_{bottom} [mA/cm^2]	Eff. [%]	Deg. [%]
160	1.36 (1.36)	77(70)	9.1 (8.7)	12.9(12.5)	9.6 (8.3)	13
220	1.27(1.25)	74(66)	9.5 (8.9)	14.9(14.6)	8.9 (7.4)	16
300	1.35(1.34)	73 (62)	10.7(10.3)	11.5(11.2)	10.5(8.6)	18
400	1.33 (1.32)	65 (59)	11.8(10.6)	13.8(13.3)	10.2(8.3)	19
600	1.25 (1.26)	58 (53)	12.1 (9.9)	11.3 (11.1)	8.2 (6.6)	19

Our tandem solar cells degrade mostly in J_{sc} and FF, similar to the single a-Si:H junction case [22]. However, FF can be strongly affected by the current density matching of the two sub cells [20,23]. Therefore, we concentrate our study on the light induced degradation of the J_{sc} of the top cell. Table 1 shows the initial and stabilized J_{sc} versus the a-Si:H top cell

thicknesses of micromorph tandem cells. The initial J_{sc} saturates at 12 mA/cm2 whereas the stable J_{sc} saturates at about 10.5 mA/cm2. This clearly limits the efficiency of the tandem device since a total current density of 23.5mA/cm^2 is presented in Table 1. Therefore, the simple tandem device optical design without IR clearly limits the cell performances to 10 % in the stabilized state assuming the best Jsc of 10.5mA/cm2 and optimistic Voc = 1.4V and FF = 70%. The mitigation of poor top cell current density is usually achieved by introducing an intermediate reflector (IR) between the a-Si:H and the μc-Si:H cells. First, we include a thin IR consisting of in-situ SiOx (SOIR) as used in the first part of the paper. However in the n-i-p configuration, the thin SiOx layer reproduces the surface texture of the bottom cell which is governed by the large feature size of the back reflector. This is clearly non optimal but the J_{top} gain can be strongly enhanced with an asymmetric intermediate reflector (AIR)[16], which not only reflects, but also scatters the light into the top cell. We realize this concept by an intermediate reflector layer of LPCVD-ZnO as shown in Figure 10. With this AIR, we obtain an efficient light in-coupling in the top cell between the AIR and the front contact. In fact, the roughness of the AIR is carried through the top cell thickness, resulting in light scattering at both, the front and the back interface of the a-Si:H top cell. Thus, our AIR consisting of thick textured ZnO deposited by LP-CVD introduces light scattering in addition to reflection at the index contrast which underlies the simple conformal IR.

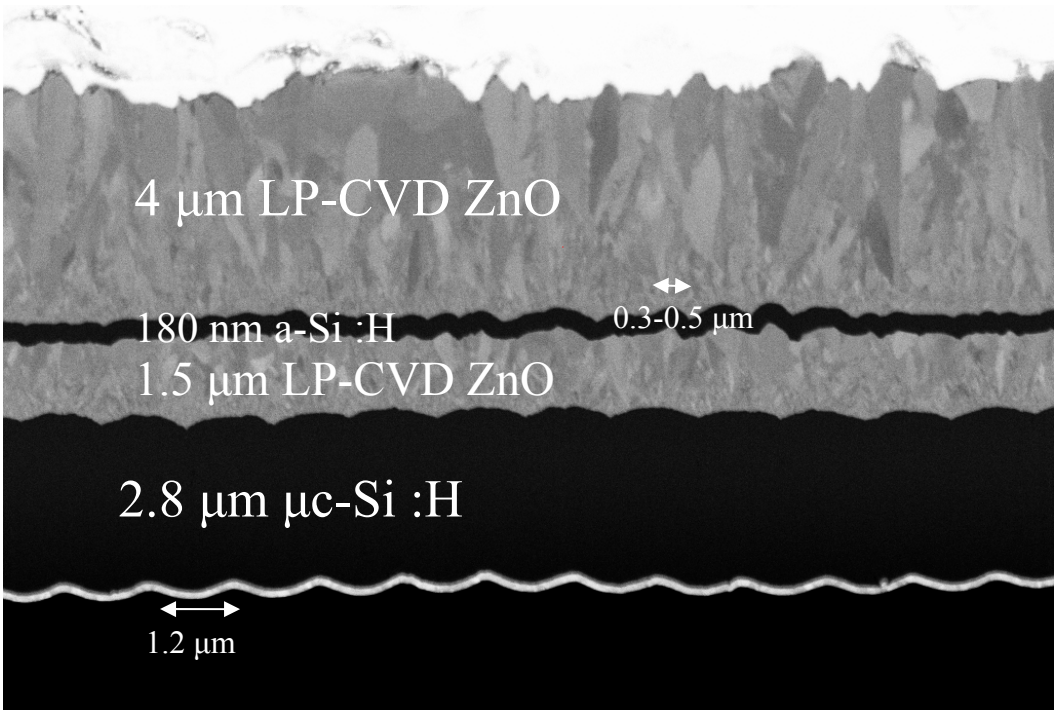

Figure 10: SEM micrographs of a cross-section of a n-i-p micromorph with AIR deposited on plastic foils.

The effect of the IRs are shown in Figure 11, where the EQE of three top a-Si:H cells of n-i-p micromorph tandem solar cells, without IR, with 100 nm thin SOIR IR with (n_{soir} = 2 @600nm) and with AIR of 1.5 μm of LP-CVD (n_{AIR} = 1.8 @600nm) are compared. All a-Si:H top cells have equal absorber thicknesses of 200 nm. The Jsc of the top cell increases with the introduction of the IR. In Figure 11, the thin IR increases the Jsc by an absolute 0.7 mA/cm^2 whereas the AIR increases the Jsc by 3 mA/cm^2. At 650 nm, the relative gain in the EQE is 60% for the thin IR and 220% for the AIR. We attribute the effect of the AIR mainly to its texture; indeed, the μc-Si:H layer even smoothes the initial substrate texture but the AIR establishes a roughness, which creates ideal light scattering for the top cell. Therefore, the light is

both reflected and scattered by the AIR. This creates light trapping in the a-Si:H top cell, sandwiched between the top front contact and the IR.

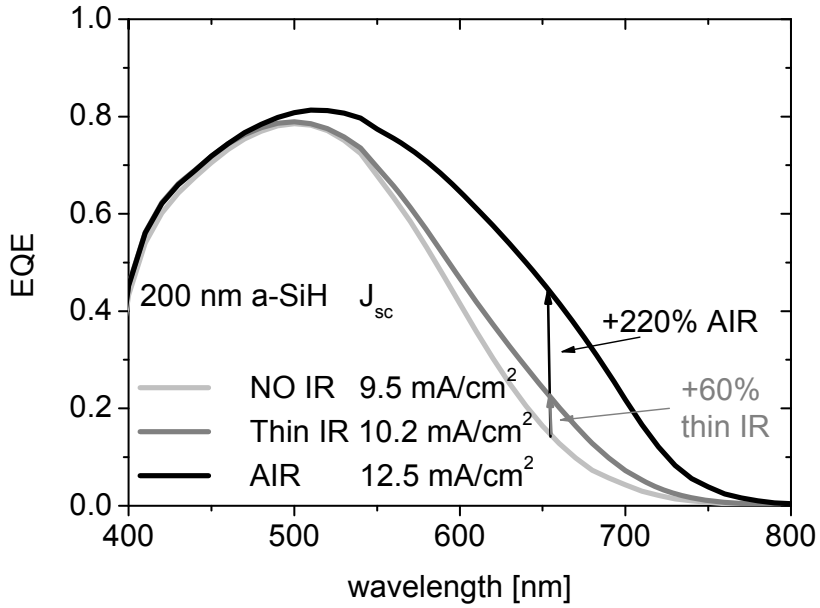

Figure 11 : EQE of 200 nm top a-Si:H in n-i-p micromorph solar cell without IR, with a thin IR (silicon oxide IR), with AIR (1.5 μm thick LP-CVD ZnO).

The AIR increases the effective thicknesses of the a-Si:H layer, which is crucial for limiting the light-induced degradation of the micromorph tandem cell. In Table 2, we compare the typical degradation for micromorph cells without IR and with AIR. The degradation is between 15-20% for a top cell of 300 nm without IR whereas the degradation is limited to 0 -10% for the a-Si:H cell thickness below 200 nm and an AIR. The results shown in Table 2 are obtained on glass covered with hot silver and a LP-CVD ZnO front contact. The results obtained with AIR in Table 2 have a stable efficiency of 9.6% with thin 1.4 μm μc-Si:H cells and 10.1% with 3 μm thick bottom cells with only 8% and 3% relative degradation, respectively.

Table 2: Performance parameters of the micromorph tandem solar cells deposited on hot silver without IR and with AIR (stabilized parameters are given in brackets).

Thickness a-Si/μm-Si [μm]	V_{oc} [mV]	FF [%]	J_{top} [mA/cm2]	J_{bottom} [mA/cm2]	Efficiency [%]	Deg. [%]
0.3/1.2 No IR	1.35 (1.34)	73 (62)	10.7 (10.3)	11.5 (11.2)	10.5 (8.6)	18
0.14/1.4 AIR	1.32 (1.34)	74 (70)	11.4 (10.3)	10.6 (10.2)	10.4 (9.6)	8
0.18/3 AIR	1.32 (1.35)	66 (65)	12.4 (11.7)	11.9 (11.5)	10.3 (10.1)	3

We deposit micromorph tandem cells with different a-Si:H cell thicknesses with and without AIR and evaluate the light induced degradation. Again, we discard bias in FF due to different matching condition and we concentrate on the light

induced degradation of the a-Si:H top cell Jsc. Figure 12 compares the J_{sc} of micromorph tandems cells with and without AIR. It shows that in the initial state, the AIR can provide J_{sc} up to 14 mA/cm2 for a 300 nm thick a-Si:H top cell, whereas a cell without IR can hardly reach more than 12 mA/cm2. In the stable state, the situation is even more critical because the Jsc with the AIR attains more than 12 mA/cm2 with only 200 nm whereas only 10.5 mA/cm2 is achieved without IR. The relative efficiency gain is close to 15% thanks to the Jsc. In addition, not only the Jsc but also the FF in stabilized state should be improved. Our experimental results confirm this efficiency gain in the stabilized state with the AIR and the best stable efficiency on hot silver substrate and on flexible substrate is 10.1 % and 9.8%, respectively.

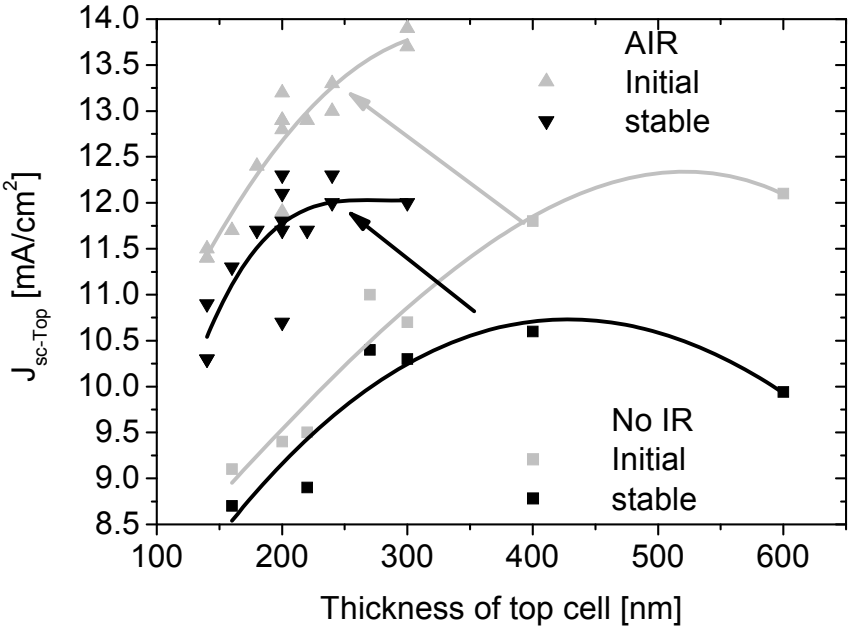

Figure 12: J_{sc} of initial and stable (1000h, 50°C and 50 mW/cm^2) micromorph tandem cells with and without AIR.

4. SUMMARY AND CONCLUSION

We report on the implementation of LP-CVD ZnO layers in thin film silicon solar cells. This transparent conductive oxide can combine high transparency (T>80%), texture adapted for light trapping (high haze and more important high scattering angle in the silicon[10]) and high conductivity (Rsq < 10 ohmsq). This is the reason why the record efficiency for a-Si:H is achieved on this substrate[24]. Its wide range of feature sizes and surface morphologies is also an advantage for the balance between the quality of silicon material grown on it, and light management in the devices. LP-CVD ZnO was used in the past mainly as TCO with the p-i-n solar cells. Here, we demonstrate that reducing the temperature to 110°C creates a film with lower resistivity and therefore also efficient as intermediate reflector. In addition, the textured film is of high interest for n-i-p micromorph tandem cell because it creates an index contrast which reflects the light in the top cell and an adapted texture which scatter the light in the top cell. We have presented devices which contain more ZnO layers (at least thicker) than silicon photoactive layers. This demonstrates the crucial role of this film in our high efficiency thin film silicon solar cell performance. Thanks to the LP-CVD ZnO, the best cells achieved in Neuchâtel have stabilized efficiencies of 11.2% and 9.8% for p-i-n cell on glass substrate and for n-i-p cell on plastic foils, respectively.

5. ACKNOWLEDGEMENTS

We thankfully acknowledge the support from the EU projects Flexcellence (contract No. 019948) and Athlet (contract No. 019670) as well as support from the Swiss Federal Office for Energy (OFEN) under project No. 101191.

6. REFERENCES

1 M. A. Green, Progress in Photovoltaics: Research and Applications **17,** 183-189 (2009).
2 A. Shah, P. Torres, R. Tscharner, N. Wyrsch, and H. Keppner, Science **285,** 692 (1999).
3 J. Meier, R. Fluckiger, H. Keppner, and A. Shah, Applied Physics Letters **65,** 860-862 (1994).
4 F. Meillaud, A. Shah, C. Droz, E. Vallat-Sauvain, and C. Miazza, Solar Energy Materials and Solar Cells **90,** 2952-2959 (2006).
5 D. L. Staebler and C. R. Wronski, Applied Physics Letters **31,** 292-294 (1977).
6 S. Benagli, J. Hoetzel, D. Borrello, J. Spitznagel, U. Kroll, J. Meier, E. Vallat-Sauvain, J. Bailat, L. Castens, P. Madliger, B. Dehbozorgi, G. Monteduro, M. Marmelo, and Y. Djeridane, Proceedings of the 24th EUPVSEC, Valencia, Spain (2008).
7 M. S. Bennett, J. l. Newton, and K. Rajan, Proc. of the 2nd PVSEC (1987).
8 D. Fischer, S. Dubail, J. A. A. Selvan, N. P. Vaucher, R. Platz, C. Hof, U. Kroll, J. Meier, P. Torres, H. Keppner, N. Wyrsch, M. Goetz, A. Shah, and K.-D. Ufert, Proc. of the 25th IEEE PVSC**,** 1053-1056 (1996).
9 K. Yamamoto, A. Nakajima, M. Yoshimi, T. Sawada, S. Fukuda, T. Suezaki, M. Ichikawa, Y. Koi, M. Goto, T. Meguro, T. Matsuda, M. Kondo, T. Sasaki, and Y. Tawada, Solar Energy **77,** 939-949 (2004).
10 D. Dominé, P. Buehlmann, J. Bailat, A. Billet , A. Feltrin, and C. Ballif, Physica Status Solidi (RRL) - Rapid Research Letters **2,** 163-165 (2008).
11 J. Bailat, D. Dominé, R. Schlüchter, J. Steinhauser, S. Faÿ, F. Freitas, C. Bücher, L. Feitknecht, X. Niquille, R. Tscharner, A. Shah, and C. Ballif, Hawaii, 2006.
12 D. Dominé, P. Buehlmann, J. Bailat, A. Billet, A. Feltrin, and C. Ballif, Valencia, 2008.
13 P. Buehlmann, J. Bailat, D. Domine, A. Billet, F. Meillaud, A. Feltrin, and C. Ballif, Applied Physics Letters **91,** 143505 (2007).
14 F.-J. Haug, T. Söderström, M. Python, V. Terrazzoni-Daudrix, X. Niquille, and C. Ballif, To be published in Sol. En. Mat. (2009).
15 S. Fay, J. Steinhauser, N. Oliveira, E. Vallat-Sauvain, and C. Ballif, Thin Solid Films **515,** 8558-8561 (2007).
16 T. Soderstrom, F.-J. Haug, X. Niquille, V. Terrazzoni, and C. Ballif, Applied Physics Letters **94,** 063501 (2009).
17 S. Nicolay, S. FayÌˆ, and C. Ballif, Crystal Growth & Design **9,** 4957-4962 (2009).
18 J. Steinhauser, L. Feitknecht, S. Faÿ, R. Schlüchter, A. Shah, C. Ballif, J. Springer, L. Mullerova-Hodakova, A. Purkrt, A. Poruba, and M. Vanecek, Proc.of the 20th European PVSEC**,** 1608-1611 (2005).
19 J. Steinhauser, Phd thesis University of Neuchâtel (2008).
20 D. Domine, Phd Thesis, Neuchâtel (2009).
21 T. Söderström, F. J. Haug, X. Niquille, and C. Ballif, Progress in Photovoltaics **17,** 165 (2009).
22 T. Soderstrom, F. J. Haug, V. Terrazzoni, and C. Ballif, accepted in Journal of Applied Physics (2009).
23 A. Nakajima, M. Ichikawa, T. Sawada, M. Yoshimi, S. Fukuda, Y. Tawada, T. Meguro, H. Takata, T. Suezaki, and M. Goto, Proc. of the 3rd World Conference PVSEC**,** 1915- 1918 (2003).
24 J. Meier, U. Kroll, E. Vallat-Sauvain, J. Spitznagel, U. Graf, and A. Shah, Solar Energy **77,** 983-993 (2004).